

## Phase Lag between Deep Cumulus Convection and Low-Level Convergence in Tropical Synoptic-Scale Systems

WINSTON C. CHAO

*Laboratory for Atmospheres, NASA/Goddard Space Flight Center, Greenbelt, Maryland*

LITAO DENG

*Applied Research Corporation, Landover, Maryland*

(Manuscript received 6 October 1995, in final form 23 July 1996)

### ABSTRACT

This study deals with the origin of the phase lag between deep cumulus convection and low-level convergence in tropical synoptic-scale systems, known since 1974. Several possible causes, including 1) propagation of the heating field, 2)  $\beta$ , 3) vertical shear of the basic flow, and 4) vertical tilt of the heat source, are examined. The last one is found to be the reason for the phase lag. The vertical tilt of the heat source occurs as a result of evolution and propagation of mesoscale convective systems within the synoptic system. During this evolution the change of vertical heating profile results in the tilt of heating field. Previous efforts of incorporating such phase lag in wave-CISK studies are commented on.

### 1. Introduction

Cho and Ogura (1974) first reported observational evidence of the fact that, contrary to the basic assumption used in the wave-CISK (whose definition is given in Chao 1995) type of treatment of convective heating [i.e.,  $Q \propto \eta(p)\omega$  where  $\omega$  is the vertical velocity at the top of the boundary layer, a measure of boundary layer convergence and  $\eta$  is a fixed vertical profile], there is a phase lag between deep convective heating and low-level convergence in synoptic-scale tropical waves. Using Reed and Recker's (1971) data to construct a composite picture of easterly waves, Cho and Ogura found that maximum low-level convergence is about one-eighth ( $\sim 475$  km) of a wavelength ahead (to the west) of the maximum deep cumulus convective heating. It should be emphasized that this phase lag is found at the synoptic scale after smaller-scale disturbances (mainly the mesoscale convective systems) have been filtered out in the compositing procedure. A similar kind of phase lag is also found in convective systems of other tropical disturbances. It is well known in mesoscale convective systems (Fig. 20 of Houze 1989). At low-levels the intense upward motion is found in front of the mesoscale precipitation maximum and mesoscale downdraft immediately behind the pre-

cipitation maximum. The phase lag between convection and low-level convergence is also found in the eastward propagating convective disturbances, consisting of one or more super cloud clusters (often only one), associated with the Madden-Julian oscillation (MJO, Madden and Julian 1971, 1972, 1994; Nakazawa 1988; Hendon and Salby 1994). In MJO the maximum convective heating is  $10^\circ$  behind (to the west) of the maximum 850-mb convergence and is  $40^\circ$ – $50^\circ$  behind the maximum 1000-mb convergence (Hendon and Salby 1994; the lag at 1000 mb is mainly due to surface friction; see Salby et al. 1994).

This important finding of phase lag has been used in attempts to alleviate the difficulties encountered in applying wave-CISK to the study of easterly waves and Madden-Julian oscillation (MJO) [see Chao (1995) for the origin of these difficulties in the MJO studies] with mixed results (Davies 1979; Cho et al. 1994). Although the scale selection problem in the wave-CISK study of MJO has to some extent been alleviated by incorporating the phase lag feature, the other problem of too high speed remains. In the meantime it creates a new problem of violating the high degree of cancellation between the convective heating and adiabatic cooling due to vertical motion (Davies 1979).

Hitherto the origin of this phase lag has not been thoroughly investigated, though association of it on the synoptic scale with the "time scale for the deep clouds to adjust themselves to reach a statistical equilibrium"

---

*Corresponding author address:* Dr. Winston C. Chao, Mail Code 913, NASA/GSFC, Greenbelt, MD 20771.  
E-mail: winston.chao@gsfc.nasa.gov

has been proposed (Cho and Ogura 1974) and some remarks about its being related to organized mesoscale system have been made (e.g., Cho et al. 1994). The purpose of this paper is to investigate the origin of this phase lag on the synoptic scale (e.g., easterly waves and super cloud clusters).

In a resting nonrotating atmosphere, if an imposed stationary heat source has no vertical tilt, the maximum low-level convergence (same as the low-level vertical velocity) is exactly in phase with the maximum vertically accumulated heating (an analog of precipitation). As explained in the following sections, such in-phase relationships can be broken by 1) relative motion of the heat source with respect to the basic atmospheric flow, 2)  $\beta$ , 3) vertical shear of the basic flow, and 4) vertical tilt in the heating distribution. We will examine these possible causes. The result of our investigation shows that the vertical tilt in the heating distribution is the cause for the phase lag and that heat source propagation leads to a phase lag of the opposite sign. Both  $\beta$  and vertical shear play negligible roles. In the atmosphere the convective heating is not prescribed but is a result of interaction with the circulation field. Thus, we will also examine the cause for the tilt. Besides these four factors we will also discuss the effect of surface friction. In addition we will comment on why, when the phase lag is introduced in the previous wave-CISK studies of MJO, it alleviated one problem and left the other problem untouched and why it created a new problem. We will start from an analytical study with a highly simplified model following the approach of Gill (1980) and Chao (1987) and demonstrate why a phase lag can result from propagating convectively forced systems. Results from Chao and Lin's (1994; hereafter CL) 2D and Chao and Deng's 3D (1995; hereafter CD) simulations of super cloud clusters and MJO will be presented to support our interpretation for the origin of the phase lag and to demonstrate the importance of the internal structure of the convective region in the successful simulation of the phase lag. The implications of this study for cumulus parameterization will be discussed.

## 2. Effects of heat source propagation

The composite studies of synoptic and planetary-scale convective systems (e.g., Cho and Ogura 1974; Madden and Julian 1972; Salby and Hendon 1994; The easterly waves have clearly a synoptic scale; whereas the MJO has a synoptic-scale convective region and a planetary-scale circulation field.) give a picture of convective circulation of simple baroclinic vertical structure. Thus, we can use a simple shallow-water equation with resting basic state as the foundation of our study. Further justification of the use of a shallow-water equation for a tropical large-scale convective system can be found in Gill (1980). Chao (1987) and Yamagata

(1987)<sup>1</sup> generalized Gill's (1980) study and obtained analytical solution for circulation forced on a  $\beta$  plane by a prescribed heating source moving at a constant speed. The solution, like that of Gill, has Kelvin wave-like and Rossby wave-like components. This solution is suitable for our present purpose and will be used. However, to isolate the effect of the Coriolis force, we will first use an even simpler analytic model. This is a model identical to Gill's but with no latitudinal dependence, no wind in the meridional direction, no Coriolis force, and no  $\beta$ . A heat source that is moved at a prescribed speed of  $C_0$  is imposed. [This model will be referred to as the 2D analytic model because it can be compared with the 2D simulation of CL. Likewise the Chao (1987) model, which will be used next, will be referred to as the 3D analytic model.]

Of course this design requires an explanation of why the heat source should move relatively to the basic flow. The answer for the super cloud cluster, which is considered by CL as the driver of MJO, has been offered by CL and Chao (1995). Briefly, a cloud cluster (a heat source) in its abrupt rise excites gravity waves, which are fairly symmetric with respect to the cloud cluster and the gravity waves trigger a new cloud cluster on the upstream (the east) side (the side where the basic flow is from and where moist content is higher than the downstream side). The new cloud cluster then triggers the next generation of cloud cluster in a chain reaction. The rising of new cloud clusters on the upstream side and the decay or poleward propagation of the existing cloud clusters give rise to an envelope, the super cloud cluster, which moves upstream. Chao and Lin (1994) interpreted the super cloud cluster as a solitary wave. For cloud clusters, the movement is due to the similar mechanism; one cloud cell sets off gravity waves to trigger another and thereby sets off a chain reaction. A similar mechanism probably operates in the easterly waves; however, the preferred propagation direction of the convective region in the easterly waves relative to the basic flow still awaits explanation.

Since no long-wave approximation (defined in Gill 1980) is used (unlike Gill's model), this model is meaningful for many different scales. The governing equations in nondimensional form are

$$-C_0 \frac{\partial u}{\partial x} + \epsilon(u + C_0) = -\frac{\partial p}{\partial x} \quad (1)$$

$$-C_0 \frac{\partial p}{\partial x} + \epsilon p + \frac{\partial u}{\partial x} = -Q \quad (2)$$

$$-w = \frac{\partial u}{\partial x}, \quad (3)$$

<sup>1</sup> Both Chao (1987) and Yamagata (1987) gave only a partial solution. The complete solution is given in Chao (1995).

where  $U$  is the zonal wind,  $p$  the surface pressure perturbation, and  $\epsilon$  the nondimensional dissipation rate. All quantities have been scaled by  $(2\beta c)^{-1/2}$  and  $[c/(2\beta)]^{1/2}$ , where  $c = (gH)^{1/2}$ ,  $g$  is the acceleration due to gravity, and  $H$  is the equivalent depth in time and length, respectively. As in Chao (1987) we will set  $c = 50 \text{ m s}^{-1}$ . This gives a length scale of  $1.07 \times 10^6 \text{ m}$  and a timescale of  $2.15 \times 10^4 \text{ s}$ . Following Gill (1980) we set  $Q = \cos(kx)$  for  $|x| < L$  and  $Q = 0$  otherwise, where  $k = \pi/2L$  and  $L$  is the half-width of the convective region. Equation (2) already indicates that if the sum of the first two terms is not in phase with either of the other two terms, there should be a phase lag between convective heating  $Q$  and low-level convergence  $\partial u/\partial x$ . If  $C_0=0$ , the governing equations have an east-west symmetry with respect to  $x = 0$  in the moving framework (assuming  $Q$  is symmetric with respect to  $x = 0$ ) and  $Q$  and  $-p$  are exactly in phase with  $-\partial u/\partial x$ . When  $C_0 \neq 0$ , this in-phase relationship is destroyed. Thus, a phase lag is a necessary outcome of the system's response to the movement of the heat source. Precisely which one of  $Q$  and  $-\partial u/\partial x$  leads the other and by what length can be ascertained by solving these equations. (It is easy to show that this phase relation is not changed by switching back to continuously sinusoidal heating as in the unconditional heating of wave-CISK.) For convenience, the following two quantities are defined:

$$q = p + (u + C_0)$$

$$r = p - (u + C_0).$$

The solutions in nondimensional form are given as follows:

$$p = \frac{1}{2}(q + r)$$

$$u + C_0 = \frac{1}{2}(q - r).$$

For  $|C_0| < 1$ ,

$$[k^2(1 - C_0)^2 + \epsilon^2]q = \begin{cases} 0, & x < -L \\ -\epsilon \cos(kx) - (1 - C_0)k \\ \quad \times \left\{ \sin(kx) + \exp\left[\frac{-\epsilon}{1 - C_0}(x + L)\right] \right\}, & |x| < L \\ -k(1 - C_0) \left[ 1 + \exp\left(\frac{-2\epsilon L}{1 - C_0}\right) \right] \\ \quad \times \exp\left[\frac{-\epsilon}{1 - C_0}(x - L)\right], & x > L. \end{cases}$$

$$[k^2(1 + C_0)^2 + \epsilon^2]r = \begin{cases} -k(1 + C_0) \left[ 1 + \exp\left(\frac{-2\epsilon}{1 + C_0}\right) \right] \\ \quad \times \exp\left[\frac{\epsilon}{1 + C_0}(x + L)\right], & x < -L \\ -\epsilon \cos(kx) + k(1 + C_0) \\ \quad \times \left\{ \sin(kx) - \exp\left[\frac{\epsilon}{1 + C_0}(x - L)\right] \right\}, & |x| < L \\ 0, & x > L. \end{cases}$$

For  $C_0 > 1$ , the solutions are

$$[k^2(1 - C_0)^2 + \epsilon^2]q = \begin{cases} k(1 - C_0) \left[ 1 + \exp\left(\frac{2\epsilon L}{1 - C_0}\right) \right] \\ \quad \times \exp\left[\frac{-\epsilon}{1 - C_0}(x + L)\right], & x < -L \\ -\epsilon \cos(kx) - (1 - C_0)k \\ \quad \times \left\{ \sin(kx) - \exp\left[\frac{-\epsilon}{1 - C_0}(x - L)\right] \right\}, & |x| < L \\ 0, & x > 0 \end{cases}$$

and  $r$  is the same as above. For  $C_0 < -1$ ,  $q$  is the same as in the case for  $|C_0| < 1$  and

$$[k^2(1 + C_0)^2 + \epsilon^2]r = \begin{cases} 0, & x < -L \\ -\epsilon \cos(kx) + k(1 + C_0) \\ \quad \times \left\{ \sin(kx) + \exp\left[\frac{\epsilon}{1 + C_0}(x + L)\right] \right\}, & |x| < L \\ k(1 + C_0) \left[ 1 + \exp\left(\frac{2\epsilon}{1 + C_0}\right) \right] \\ \quad \times \exp\left[\frac{\epsilon}{1 + C_0}(x - L)\right], & x > L. \end{cases}$$

Figure 1 shows the distribution of  $Q$  and  $w (= -\partial u/\partial x)$  for  $L = 1$  ( $\sim 1000 \text{ km}$ ),  $\epsilon = 0.25$ ,  $C_0 = 0.2$  ( $\sim 10 \text{ m s}^{-1}$ ), which is a typical speed of convective system relative to the easterly basic flow. It shows that convergence lags convective heating by (when converted to dimensional units) about 150 km, a situation opposite to what is observed in the real atmosphere. This phase lag of the opposite sense can be understood this way. In the framework moving with the heat source, the

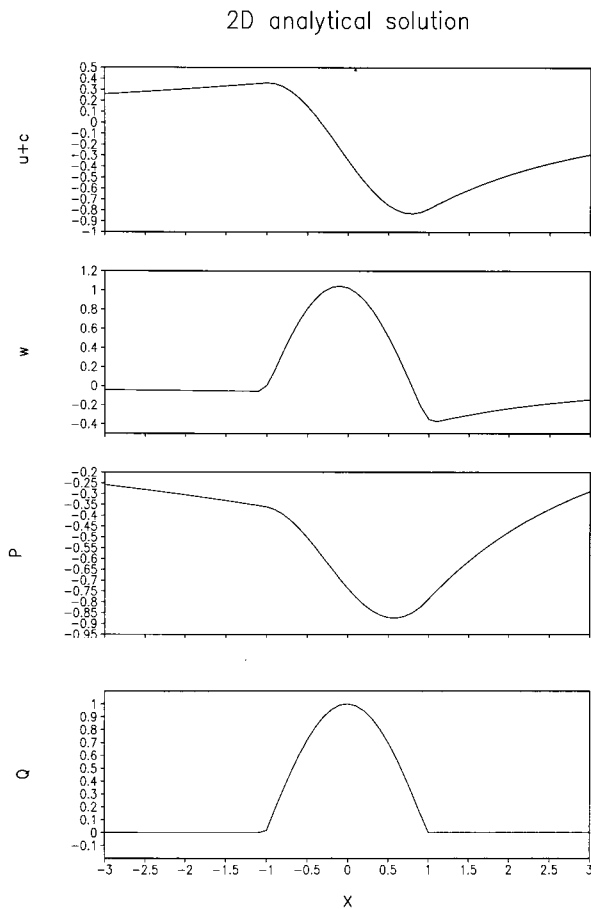


FIG. 1. Horizontal distributions of nondimensional  $u + c$ ,  $w$ ,  $p$ , and  $Q$  for the 2D analytic model for the case of  $L = 1$ ,  $C_0 = 0.5$ , and  $\epsilon = 0.25$ .

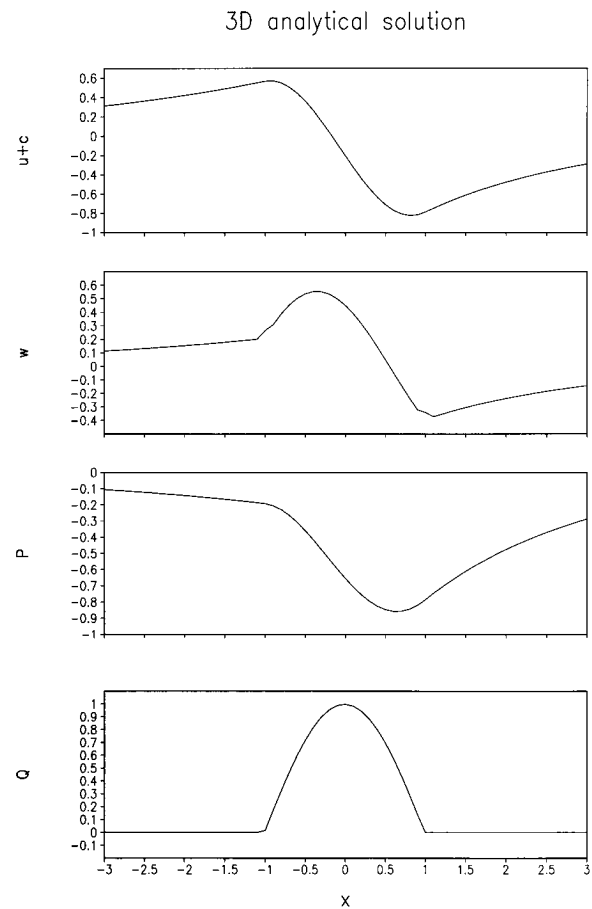


FIG. 2. Same as in Fig. 1 except for the 3D analytic model along the equator.

steady state requires a larger upward motion behind (rather than ahead of) the heat source maximum to balance the positive contribution from the horizontal temperature advection.

### 3. Effect of $\beta$

The above analysis shows that the symmetry with respect to the convective heating source is broken when the heat source moves with respect to the basic flow, and the phase lag between low-level convergence and convective heating is a manifestation of the broken symmetry. However, this broken symmetry is of the wrong sign. The symmetry can also be broken by other means such as  $\beta$  and vertical shear in the basic flow; their significance in generating the phase lag should also be examined. We will now consider the 3D case to investigate how introducing  $\beta$  affects the picture. For cloud-scale and cloud cluster-scale systems  $\beta$  is not important, thus we can consider only super cloud cluster scale, for which Gill's model is suitable. We will use Gill's model and compare its solutions for a case where the imposed heat source is stationary and a case where the imposed

heat source is moving. The governing equations for the 3D case are given in Chao [1987, see his Eq. (1)–(4)] and the complete solution is given in Chao (1995). Figure 2 is for the case identical to that of Fig. 1 except for the 3D analytic model; it presents the solution at the equator for  $C_0 = 10 \text{ m s}^{-1}$ . It shows hardly any difference from Fig. 1. Figure 3 is the same case as that of Fig. 2 except that  $C_0$  is zero. Figures 2 and 3 demonstrate that  $\beta$  alone without the help of  $C_0$  generates almost no phase lag between convective heating and low-level convergence. The impact of vertical shear in the basic flow will be presented in the next section when we deal with the multilevel model.

Thus, our basic conclusion based on our simple analytic models is that the phase lag between convective heating and low-level convergence is not caused by  $\beta$  or the dynamical response of the system to the propagation of the heat source with respect to the basic flow.

Although we have no doubt about the basic conclusion from this simple analytic study using a shallow-water equation that the cause for the phase lag is not the propagation of the heat source, we should point out a fundamental limitation of the present analytic model.

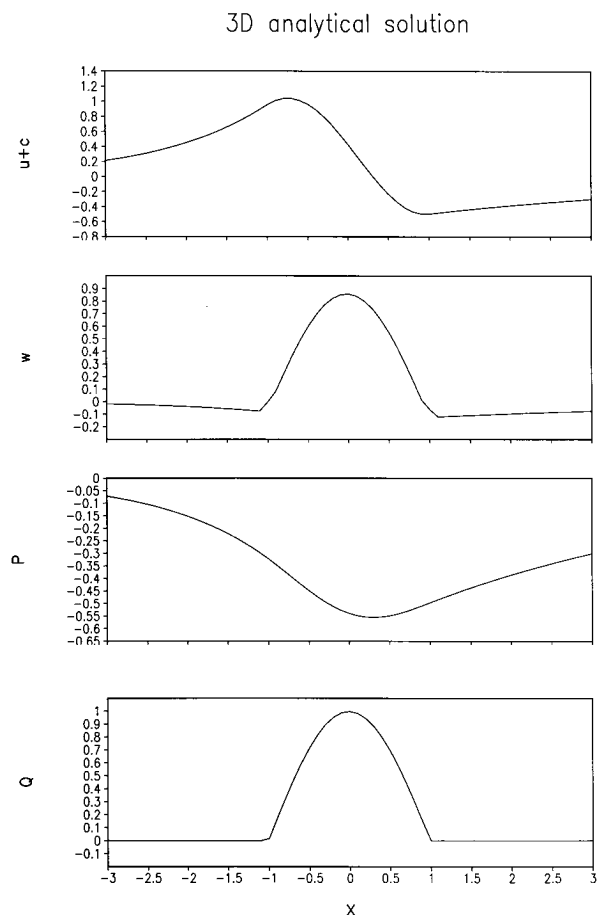


FIG. 3. Same as in Fig. 2 except for  $C_0 = 0$ .

The shallow-water equation, besides its capability of modeling barotropic phenomena, can be, as in our study, used as a simplified two-level model (Gill 1980). The analytic solutions given above are considered as those of the lower level and those of the upper level are simply the same ( $u + C_0$ ),  $p$ ,  $v$ , and  $Q$  but with a minus sign added to each. The obvious limitation of such a two-level model is that it cannot have vertical tilt in vertical velocity. Thus, to get a more complete picture we have to go to models with more levels. In the next section we will discuss results from CL's and CD's multilevel models.

#### 4. Effects of vertical shear

To investigate the effects of the vertical shear of the basic flow, we will use CL's 2D (height and longitude) model. The 2D model is a north-south compression of the Goddard Laboratory for Atmospheres general circulation model (GLA GCM). There is no meridional wind or Coriolis force in the 2D model. The details of the model can be found in CL and here we will give a very brief description. The model's dynamics is that of the GLA GCM. The radiation package is replaced by a

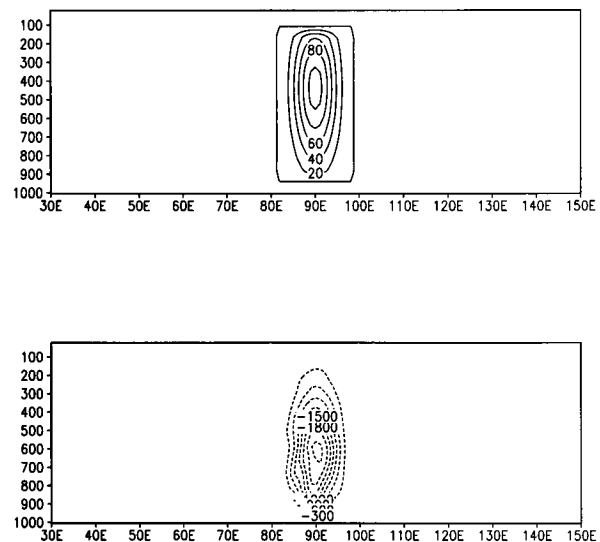


FIG. 4. The composite vertical structure of the fields in a convectively forced circulation in a sheared basic flow: showing (a) the prescribed stationary heating in  $(10^{-1} \text{ } ^\circ\text{C day}^{-1})$ , (b), the vertical  $p$  velocity  $(10^{-6} \text{ mb s}^{-1})$ . The vertical axis shows the model level numbers, whose pressure values are given in Table 1.

prescribed cooling rate as a function of height only. The turbulence and boundary layer parameterization are those of the ECMWF model (Louis 1979), and the cumulus parameterization is that of Manabe et al. (1965). The bottom surface is ocean with a uniform SST of  $30^\circ\text{C}$ . To ensure the basic flow in the 2D model has a shear, the zonal flow is forced by instantaneous restoration of the zonal mean zonal wind to a preset linear shear flow of  $5 \text{ m s}^{-1}$  at the top level and  $-5 \text{ m s}^{-1}$  at the bottom level. The 2D model has a longitudinal domain of  $180^\circ$  and uses cyclic boundary condition.

The model experiment is conducted with a prescribed stationary heating pattern with no vertical tilt. All surface fluxes are set to be zero. Figure 4 shows the prescribed heating field ( $10^{-1} \text{ } ^\circ\text{C day}^{-1}$ ) and the time-averaged results of the last 20 days of a 90-day run. The results show little tilt in the vertical velocity field ( $10^{-6} \text{ mb s}^{-1}$ ). Thus, vertical shear in the basic flow cannot explain the synoptic-scale phase lag between deep convection and low-level convergence.

#### 5. Effects of the vertical tilt of heating field

The existence of the vertical tilt in the heating field for the easterly waves can be inferred from Fig. 8b of Reed and Recker (1971), which shows a tilt with height toward the rear (the east) in the vertical velocity field. The high degree of cancellation in the Tropics between convective heating and adiabatic cooling due to upward motion implies that a tilt exists in the convective heating field.

To investigate the effects of the tilt in the heating field, we will again use CL's 2D model. Before we in-

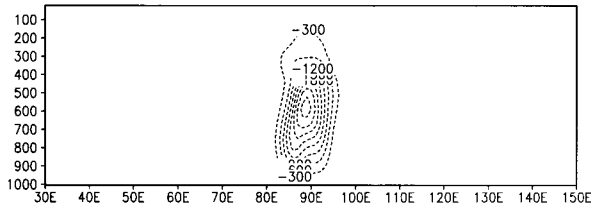


FIG. 5. The composite vertical structure of the vertical  $p$  velocity ( $10^{-6}$   $\text{mb s}^{-1}$ ) in a resting basic flow forced by a moving heating field shown in Fig. 4a, viewed from a coordinate moving with the heating field.

investigate the CL and CD model results, we will use the CL's 2D model in a study similar to what was presented in the preceding section; that is, the study of the circulation response to a prescribed heating source. In these sets of experiments the entire model physics component is replaced by a prescribed heat source of a horizontal scale of  $20^\circ$  with no vertical tilt moving at  $10 \text{ m s}^{-1}$ . All surface fluxes are set to be zero. The basic zonal mean flow is restored to zero at all levels at every time step. An advantage of this treatment of mean flow is that there is no vertical shear in the basic flow to be concerned about. Figure 5 shows the time-averaged results in a coordinate moving with the heat source. The results show a phase lag between heating and low-level convergence consistent with the results in section 2.

A more important experiment is one in which the heating field is not prescribed and is a product of the cumulus parameterization (Manabe et al. 1965) used in the model. In this experiment the basic zonally averaged zonal wind is restored to  $-5 \text{ m s}^{-1}$  at every time step. Figure 6 shows the composite picture in such an experiment with the CL model. The method of compositing is first shifting the model result in the longitudinal direction, and the amount of shifting is a linear function of time such that the super cloud cluster becomes stationary. (As a minor point, this is not completely the same as viewing the system from a coordinate moving with the super cloud cluster in the sense that the speed of the super cloud cluster is not subtracted from the zonal wind field.) Figure 7 shows schematic diagrams of the super cloud cluster before and after the shift. This shifting is followed by a time average to get the composite picture of the super cloud cluster. The precipitation distribution (inferred from Fig. 6a) in the super cloud cluster shows a higher gradient on the western side than on the eastern side. There is a westward tilt with height of about  $1 \text{ km mb}^{-1}$  in the circulation field. In association with this tilt the maximum low-level convergence is ahead of the maximum precipitation by about 400 km in agreement with observation. The composite convective heating field is a mixture of the convective heating in the cloud cluster and the zero convective heating between the cloud clusters (Fig. 7b). Moving from east to west in Fig. 6a, we follow the life cycle of the average cloud cluster. Initially the vertical heating profile does not show a distinct maximum. As

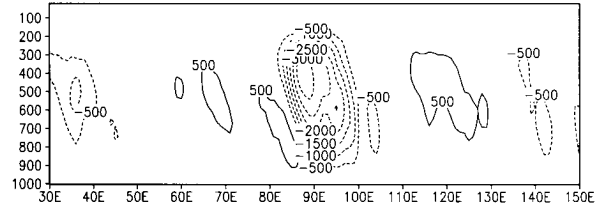
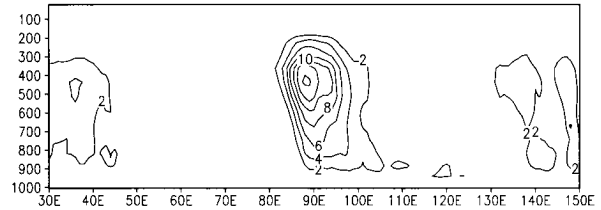


FIG. 6. The composite vertical structure of the super cloud cluster that appears in the CL model showing: (a) the diabatic heating field ( $^\circ\text{C day}^{-1}$ ), (b) the vertical  $p$  velocity ( $10^{-6}$   $\text{mb s}^{-1}$ ).

the cloud cluster develops, the vertical heating profile changes to give a distinct maximum at the 400-mb level. It is such life cycle that gives rise to the tilt in the heating field. Our results compare well with observations (Houze 1982), which show that the maximum heating level in a cloud cluster moves upward as it matures. To arrive at an explanation for such evolution requires a study of the life cycle of the cloud clusters and this will be pursued in a separate study.

We have also obtained the same vertical tilt in our 3D modeling of the super cloud clusters. The 3D model is a global aqua-planet model and the SST is a function of latitude only. The radiative cooling rate is a prescribed function of latitude and height. The basic zonally averaged flow is self-generated, just like in any common GCM. Figure 8 shows the height–longitude composite (last 20 days of a 60-day simulation) of convective heating and vertical velocity along the equator. It shows the same kind of vertical tilt ( $\sim 1 \text{ km mb}^{-1}$ ) as in the 2D

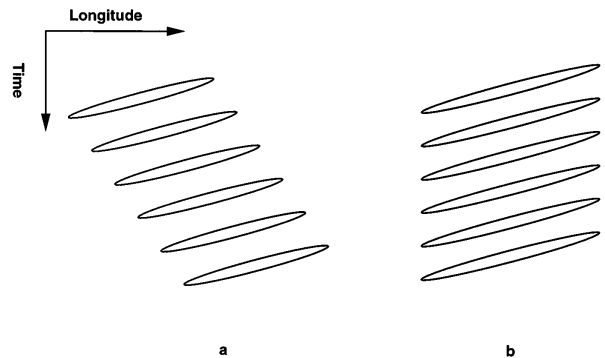


FIG. 7. A schematic diagram showing the super cloud cluster (a) before and (b) after the shifting in the compositing procedure.

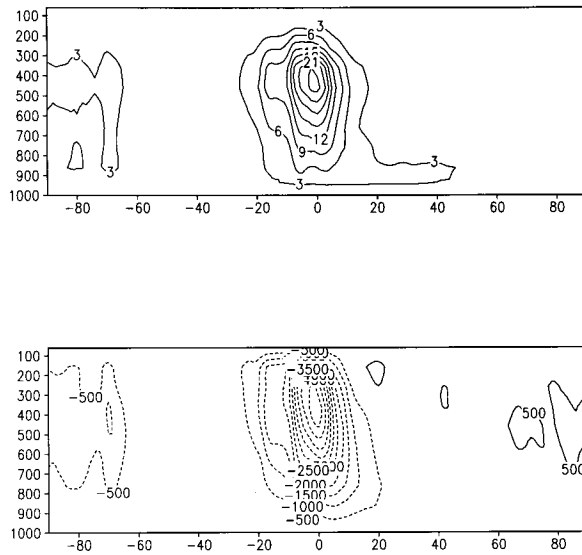


FIG. 8. The composite vertical structure of the super cloud cluster along the equator that appears in the 3D model: (a) the diabatic heating field ( $^{\circ}\text{C day}^{-1}$ ), (b) the vertical  $p$  velocity ( $10^{-6} \text{ mb s}^{-1}$ ).

model indicating a phase lag between the deep convection and the low-level convergence of the same magnitude.

The picture in the 2D model is different from that in the 2D analytic model. In the latter model, when considered as a representation of a two-level model, the upper-level maximum divergence is directly above the low-level convergence. In the 2D model, the upper-level maximum divergence is to the west of the low-level convergence.

The phrase vertical tilt may not be the best phrase to describe the heating pattern in our 2D super cloud cluster. If we take the heating field used in the experiments reported in the preceding section and simply tilt it, the heating profile in the initial phase of the cloud cluster, instead of being fairly uniform, will be limited to the lower troposphere. However, since such tilt is enough to generate the phase lag between deep convection and low-level convergence, we will keep using the phrase vertical tilt when explaining the cause for the phase lag (a possible alternative but more vague term may be the evolution of cloud cluster vertical heating profile).

To lay background for the discussions in section 7, we will now present an analysis of the 2D model heat budget. The thermodynamic equation in a coordinate system moving with the super cloud cluster has the following form:

$$[u - C_0] \frac{\partial [T]}{\partial x} + \left[ u' \frac{\partial T'}{\partial x} \right] + [\omega] \left( \frac{\partial [T]}{\partial p} - \frac{[\alpha]}{C_p} \right) + \left[ \omega' \left( \frac{\partial T'}{\partial p} - \frac{\alpha'}{C_p} \right) \right] = \frac{[Q]}{C_p}, \quad (4)$$

where  $u$  is the zonal velocity in the fixed coordinate,  $C_0$

the speed of the super cloud cluster, the square bracket is the time mean operator reflecting the synoptic-scale field, and the prime denotes the deviation from the time mean reflecting the mesoscale eddy. The other notations are standard. Figure 9 shows the left-hand-side terms of (4) and their sum, which compares well with the right-hand-side term of (4) (Fig. 6a). The first two terms are minor. The fourth term represents the contribution from the cloud cluster (or the mesoscale) circulation and it has higher concentration in the upper troposphere. In a synoptic-scale picture, in the sense that smaller-scale circulation is filtered out, the sum of the fourth and the right-hand-side term in (4) should be considered as the convective heating. At the synoptic scale it is this sum that balances the vertical adiabatic cooling (the third term) and both have the same vertical tilt. Also, it is this sum that should be parameterized in coarse-grid models that do not resolve cloud clusters. This analysis is a little different from the analysis based on the spatial average.

## 6. The effect of surface friction

Surface friction obviously directly affects the circulations in the boundary layer. The fact that the top of boundary layer has to be matched to the bottom of the free atmosphere indicates that friction has an indirect influence on the circulations in the free atmosphere. In a resting basic flow without  $\beta$ , movement of the heating field, or vertical tilt in the heating field, surface friction cannot generate any phase lag between convective heating and convergence in either the boundary layer (typically the bottom 500 m) or the lower free atmosphere (750–950 mb). Thus, if surface friction can contribute to a phase lag, it has to act in concert with other factors. The experiments in the last two sections were conducted with surface friction. To identify the role of surface friction in the phase lag between deep convection and the low-level convergence, we conducted an experiment with our 2D model in which the surface friction is set to be zero.

Figures 10 and 11 show time–longitude distribution of precipitation for the cases with and without surface friction, respectively. These two figures show that without surface friction the super cloud cluster can still exist. With surface friction the super cloud cluster structure exhibits a simple wave packet internal structure; whereas, without surface friction the super cloud cluster exhibits a more complex structure—as if there are several wave packets packed close to one another (the reason for such structure is an open question). Such structure is also seen in Fig. 12, which shows the composite vertical structure of the heating field and the vertical velocity of the case without surface friction. Corresponding to several wave packets there are several maxima in the two fields. The vertical tilt in both fields (of the same magnitude as in the case with surface friction) still exist in the case without surface friction. Thus, we have demonstrated that in the 2D model the phase lag be-

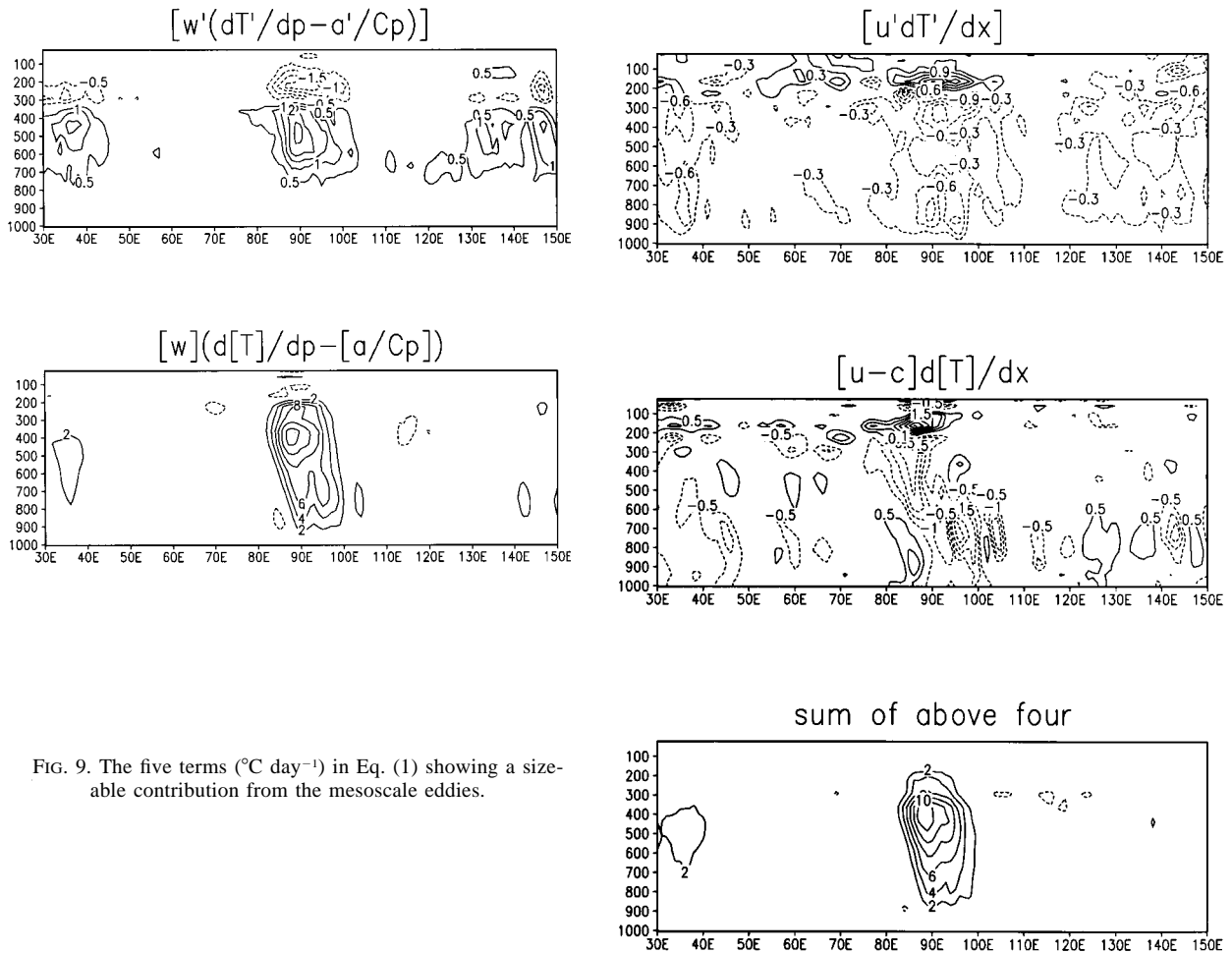


FIG. 9. The five terms ( $^{\circ}\text{C day}^{-1}$ ) in Eq. (1) showing a sizeable contribution from the mesoscale eddies.

tween deep convection and low-level convergence does not have to depend on surface friction. In a 3D situation, Hendon and Salby (1994) have demonstrated from observation that maximum convergence in the boundary layer is far ( $40^{\circ}$ – $50^{\circ}$ ) to the east of the deep convection and the convergence at 850 mb is only  $10^{\circ}$  away from the deep convection. The large phase lag in the boundary layer has been demonstrated by Salby et al. (1994) to be a result of surface friction. Obviously, the vertical motion created by the boundary layer convergence at the location of maximum boundary layer convergence is met by divergence in the free atmosphere and generates no convection. Therefore, we can conclude that as far as the phase lag that we are discussing is concerned, surface friction has contribution only in the boundary layer and plays little role in the free atmosphere.

**7. Implication for cumulus parameterization and comments on the previous applications of the phase lag to wave-CISK study**

It is not correct, on the synoptic scale, to relate the convective heating to the low-level convergence (which

by now is obvious). However, whether relating the convective heating to the phase-lagged low-level convergence is a good idea requires careful investigation. The previous attempts in wave-CISK studies of adopting the phase lag retained the heating formula of  $Q \propto \eta(p)\omega$  but  $\omega$ , the low-level vertical velocity, is taken from that at a phase-lagged position. Such implementation has the obvious deficiency of not allowing a vertical tilt in the heating field. It is clear from the above simulation results that, on super cloud cluster scale, the convective heating is an average of convective heating on cloud cluster scale, which is related to the low-level convergence at the cloud cluster scale. If one must relate the convective heating to the phase-lagged low-level convergence, one should at the same time include in the parameterization scheme the convergence of vertical eddy heat flux (from eddies of cloud cluster scale), which has not been attempted thus far. (This is an often-mentioned point that in global models, which do not resolve mesoscale systems; the cumulus parameterization should include the effects of the mesoscale convection.) Even this correctional step gives no assurance of success (not to mention the difficulty in choosing the magnitude of the lag,



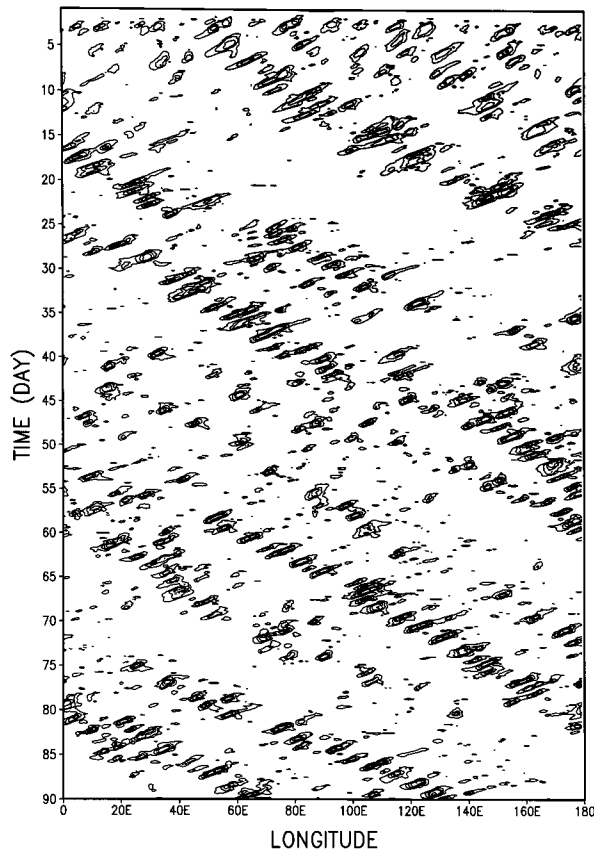


FIG. 10. Time-longitude distribution of precipitation in an experiment with the 2D model (corresponding to Fig. 6). The contour levels are 5, 20, 50, 100, 200 mm day<sup>-1</sup>.

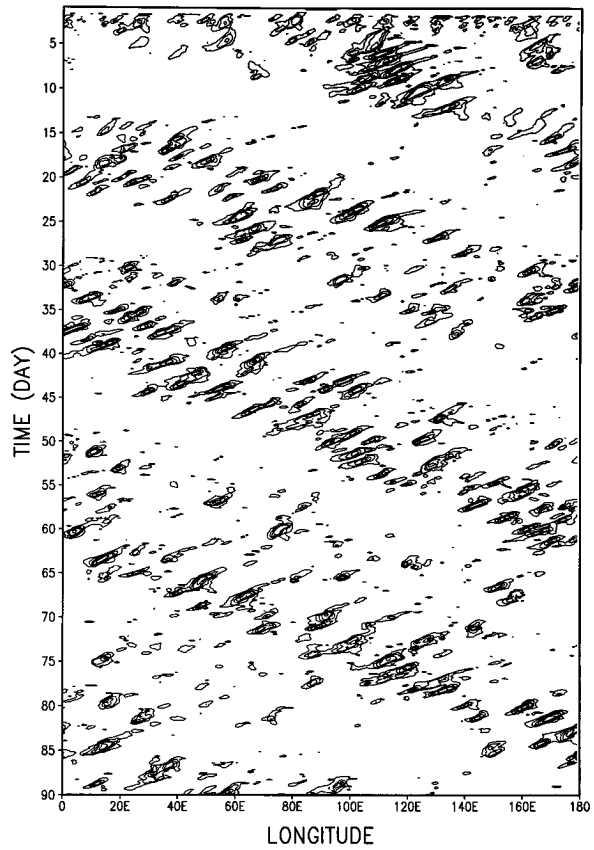


FIG. 11. Same as in Fig. 10 but for an experiment without surface friction.

which undoubtedly varies during the life cycle of the synoptic-scale convective system and is highly dependent upon the type of convective system). The convective heating on the super cloud scale (i.e., the convective heating in GCMs that do not resolve mesoscale) is associated or correlated with the phase-lagged low-level convergence. However, correlation does not necessarily imply causality. The argument that the low-level convergence provides mass flux into the cumulus may be correct on the cloud scale (That is not to say that the cloud-scale heating is caused by the low-level convergence. It is caused by convective instability.) but it is a hollow one on the synoptic scale. On the synoptic scale, the cloud mass flux at the top of the boundary layer often exceeds that supplied by the low-level convergence (Cho and Ogura 1974) even when the phase lag is taken into account. Lacking the knowledge of parameterizing mesoscale convection, our best hope at present is to use a smaller grid size and resolve the mesoscale convection as was done in CL. Admittedly, this approach is not feasible at present for multiyear GCM simulations. Another problem yet to be addressed is that of how well the mesoscale convective system

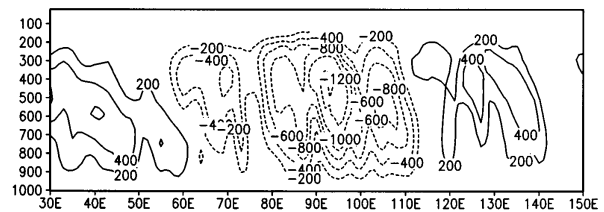
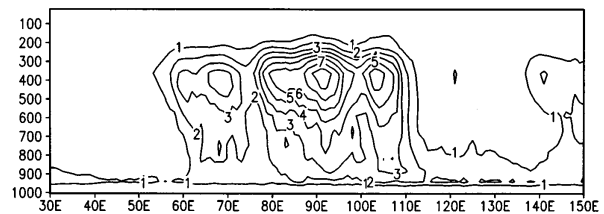


FIG. 12. Same as in Fig. 6 but for an experiment without surface friction.

should be resolved in order to simulate synoptic-scale convective systems well.

With the hindsight of this study, we can understand how inadequate the currently available cumulus parameterization schemes, that are used for coarse grid (grid size  $2^\circ \times 2.5^\circ$  and larger) GCMs, are. They are mostly patterned after some cloud models with no consideration for the mesoscale circulation parameterization. The terminology "cumulus parameterization" should be used carefully. In coarse-grid GCMs, since mesoscale convective systems are not resolved, what needs to be parameterized is not just cumulus convection but also mesoscale convection (Moncrieff 1992). Thus, the terminology "cumulus parameterization" is not appropriate for coarse-grid GCMs. A better terminology would be "subgrid-scale convection parameterization." However, even this terminology is not ideal. A process in a model should be covered by ten or a dozen grids in order to be simulated well. Those processes that have scales of only two or three grids are definitely not well simulated and they need the help of parameterization also. "Parameterization of subgrid-scale convection and poorly resolved convection" seems to be a more precise terminology. These considerations, of course, point out the complicated nature of the convection parameterization problem.

With the above consideration on convection parameterization for global-scale models, we can gain some insight into the previous attempts to incorporate phase-lagged convection in wave-CISK studies. Davies (1979) incorporated the phase lag feature in a study of wave-CISK. He found that the benefits of adding the phase-lag feature (overcoming the scale-selection problem) are overshadowed by the lack of high degree of cancellation between the convective heating and the adiabatic cooling due to large-scale upward motion. Such lack of cancellation is not surprising. The convective heating used in the wave-CISK type of studies [ $Q \propto \eta(p)\omega$ , where  $\eta$  is a fixed vertical heating profile and  $\omega$  the phase-lagged low-level vertical velocity] does not allow vertical tilt of the heating distribution; thus, when heating is phase-shifted from the low-level convergence, maximum heating is out-of-phase with the vertical velocity (at least at low-levels) and therefore the high degree of cancellation between the two contributions cannot be achieved. The results presented above from the CL model, which shows that both vertical motion and the convective heating distribution have a vertical tilt, thus a high degree of cancellation can be achieved and at the same time the results exhibit a phase lag between convective heating and the low-level convergence. The incorporation of the phase-lagged convection into wave-CISK study of the Madden-Julian oscillation (Cho et al. 1994) have alleviated the problem of scale selection. However, the excessive propagation speed remains a problem. Chao (1995) has demonstrated that the speed of the wave-CISK type analysis results is dictated by the speed that generates the maximum low-level con-

vergence into the convective heating area, because of the dependence of convective heating on the low-level convergence and this speed turns out to be very close to that of the internal Kelvin wave. Apparently, judging from Cho et al.'s results of too high speed, this situation is not changed by adding the phase-lag feature. The details of this should still be further investigated. However, we would like to point out that the convective heating used in Cho et al. (1994) is the same as in Davies (1979) in that the heating formulation,  $Q \propto \eta(p)\omega$ , does not allow a vertical tilt in its distribution due to the fixed vertical heating profile used in wave-CISK. Also, as we have discussed before, relating convective heating to low-level convergence, whether phase-lagged or not and whether the tilt in the heating field is incorporated or not, is not a physically correct way of handling convective parameterization. A correct way, including an implicit representation of the mesoscale convective systems, that can be easily used in analytic or simplified numerical studies, has yet to be found.

## 8. Summary and remarks

This study examines several possible causes for the synoptic-scale phase lag between deep convection and low-level convergence. Among them the propagation of the heat source,  $\beta$ , and vertical shear of the basic flow are found to be giving either a lag of wrong sign or of insignificant magnitude. The vertical tilt of the convective heating field is found to be responsible for the phase lag. The origin of the vertical tilt in the heat source is related to the propagation and evolution of the mesoscale convective systems within the synoptic-scale convective region. During the evolution and propagation, the vertical heating profile of the mesoscale system changes shape from a more or less uniform distribution to a distribution showing a more distinct maximum at upper levels. Such change creates the vertical tilt.

Our interpretation of the phase lag between convective heating and low-level convergence is reasonable for synoptic-scale systems such as easterly waves and super cloud clusters. For MJO, whose convective region contains one or more super cloud clusters, our interpretation is also relevant in explaining the phase lag between the convective heating and the 850-mb convergence. The  $40^\circ$ – $50^\circ$  phase lag between the convective heating and the 1000-mb convergence in the MJO (Hendon and Salby 1994), simulated in our super cloud cluster results, is due to surface friction (Salby et al. 1994).

The previous attempts in incorporating the phase-lag relation into the wave-CISK studies alleviated the problem of scale selection but they had the undesirable consequences of failing to achieve the high degree of cancellation between convective heating and the adiabatic cooling due to the large-scale upward motion. Such failure is due to the fact the heating formulation used in these wave-CISK studies does not allow vertical tilt in the heating field. The other problem of too high speed,

that remains, is related to the dependence of heating on the low-level vertical velocity. Thus, we can conclude that so-called phase-lagged wave-CISK fails to resolve the problems of wave-CISK and the cause for the failure is not being able to come up with a correct treatment of subgrid-scale convection.

This study has also clearly revealed the inadequacy of the currently available cumulus parameterization schemes for coarse-grid (grid size  $2^\circ \times 2.5^\circ$  and larger that cannot resolve the mesoscale circulation) GCMs, which do not attempt to parameterize the mesoscale convection. The need for a convection scheme that does take into account both cumulus convection and mesoscale convection will exist as long as coarse-grid GCMs are in use (for multiyear or multidecade climate simulations). A concise version of such a scheme, suitable for analytic and simplified numerical studies of synoptic- and planetary-scale phenomena, is also greatly needed and is yet to be found. And these needs pose a good challenge.

*Acknowledgments.* This work was supported by NASA Mission to Planet Earth division with funds managed by Kenneth Bergman and Ramesh Kakar as a part of NASA's participation in TOGA COARE.

#### REFERENCES

- Chao, W. C., 1987: On the origin of the tropical intraseasonal oscillation. *J. Atmos. Sci.*, **44**, 1940–1949; Corrigendum, **45**, 1832.
- , 1995: A critique of wave-CISK as the explanation for the 40–50 day tropical intraseasonal oscillation. *J. Meteor. Soc. Japan*, **73**, 677–684.
- , and S.-J. Lin, 1994: Tropical intraseasonal oscillation, super cloud clusters, and cumulus convection schemes. *J. Atmos. Sci.*, **51**, 1282–1297.
- , and L. Deng, 1995: On the origin of the Madden–Julian oscillation. Preprints, *21st Conf. on Hurricane and Tropical Meteorology*, Miami, FL, Amer. Meteor. Soc., 156–157.
- Cho, H.-R., and Y. Ogura, 1974: A relationship between cloud activity and the low-level convergence as observed in Reed–Recker's composite easterly waves. *J. Atmos. Sci.*, **31**, 2058–2065.
- , K. Fraedrich, and J. T. Wang, 1994: Cloud clusters, Kelvin wave-CISK, and the Madden–Julian oscillations in the equatorial troposphere. *J. Atmos. Sci.*, **51**, 68–76.
- Davies, H. C., 1979: Phase-lagged wave-CISK. *Quart. J. Roy. Meteor. Soc.*, **105**, 325–353.
- Gill, A. E., 1980: Some simple solutions for heat-induced tropical circulation. *Quart. J. Roy. Meteor. Soc.*, **106**, 447–462.
- Hendon, H. H., and M. L. Salby, 1994: The life cycle of the Madden–Julian oscillation. *J. Atmos. Sci.*, **51**, 2225–2237.
- Houze, R. A., 1982: Cloud clusters and large-scale vertical motions in the Tropics. *J. Meteor. Soc. Japan*, **60**, 396–409.
- , 1989: Observed structure of mesoscale convective systems and implications for large-scale heating. *Quart. J. Roy. Meteor. Soc.*, **115**, 425–461.
- Louis, J.-F., 1979: A parametric model of vertical eddy fluxes in the atmosphere. *Bound.-Layer Meteor.*, **17**, 187–202.
- Madden, R. A., and P. R. Julian, 1971: Detection of a 40–50 day oscillation in the zonal wind in the tropical Pacific. *J. Atmos. Sci.*, **28**, 702–708.
- , and —, 1972: Description of global scale circulation cells in the tropics with a 40–50 day period. *J. Atmos. Sci.*, **29**, 1109–1123.
- , and —, 1994: Observations of the 40–50-day tropical oscillation—A review. *Mon. Wea. Rev.*, **122**, 814–837.
- Manabe, S., J. Smagorinsky, and R. F. Strickler, 1965: Simulated climatology of a general circulation model with a hydrological cycle. *Mon. Wea. Rev.*, **93**, 769–798.
- Moncrieff, M., 1992: Organized convective systems: Archetypal dynamical models, mass and momentum flux theory, and parameterization. *Quart. J. Roy. Meteor. Soc.*, **118**, 819–850.
- Nakazawa, T., 1988: Tropical super clusters within intraseasonal variations over the western Pacific. *J. Meteor. Soc. Japan*, **66**, 823–839.
- Reed, R. J., and E. E. Recker, 1971: Structure and properties of synoptic-scale disturbances in the equatorial western Pacific. *J. Atmos. Sci.*, **28**, 1117–1133.
- Salby, M. L., and H. H. Hendon, 1994: Intraseasonal behavior of clouds, temperature, and motion in the tropics. *J. Atmos. Sci.*, **51**, 2207–2224.
- , R. R. Garcia, and H. H. Hendon, 1994: Planetary-scale circulations in the presence of climatological and wave-induced heating. *J. Atmos. Sci.*, **51**, 2344–2367.
- Yamagata, T., 1987: A simple moist model relevant to the origin of intraseasonal disturbances in the Tropics. *J. Meteor. Soc. Japan*, **65**, 153–164.